

Enabling the Analysis of Topologically Connected Multi-Patch Trimmed NURBS Shells in LS-DYNA

Stefan Hartmann¹, Lukas F. Leidinger^{2,3}, David J. Benson⁴,
Liping Li⁴, Attila P. Nagy⁴, Marco Pigazzini⁴

¹DYNAMore GmbH
Industriestr. 2, 70565 Stuttgart, Germany
e-mail: stefan.hartmann@dynamore.de

²TUM Department of Civil, Geo and Environmental Engineering, Technical University of Munich
Arcisstr. 21, 80333 Munich, Germany

³BMW Group Research and Innovation Center
Knorrstr. 147, 80788 Munich, Germany

⁴Livermore Software Technology Corporation (LSTC)
7374 Las Positas Road, Livermore, CA 95411, USA

1 Introduction

In 2005, the term “Isogeometric Analysis” (IGA) was introduced by Hughes et al. [1]. Since then, reams of scientific research work has been devoted to this new finite element technology, whose main idea is to use the same geometrical description during the finite element analysis (FEA) that was previously used during the design process in the computer-aided design (CAD) environment. The most widely used and best understood mathematical description in CAD is based on non-uniform rational B-splines (NURBS). Hence NURBS-based shell and solid finite elements have been developed and implemented into LS-DYNA over the last few years. Although NURBS-based solids are available, the remainder of the paper will exclusively focus on isogeometric shell element formulations in LS-DYNA.

In case of NURBS shells, thin-shell elements based on the Kirchhoff-Love shell theory as well as shear deformable shell elements based on the Reissner-Mindlin shell theory are available. LS-DYNA allows to perform finite element analysis on surface geometry descriptions based on trimmed NURBS and supports many other features that are commonly used, like contact boundary conditions, a huge library of material models, implicit and explicit time integration, mass scaling, eigenvalue analysis and others.

Within the CAD environment, the geometry of a part is typically defined by a so-called boundary representation (B-Rep). This means, that a standard NURBS patch definition is expanded by a definition of various trimming curves that define visible and invisible regions of a surface. Thus, the outer surface is defined through an underlying NURBS patch description together with a set of outer trimming curves (boundary loop) living on the patch. Furthermore specific topology information is embedded in the CAD database to specify whether two or more trimmed patches represent a connected part or not. While in the CAD world it is sufficient to simply know the topological connection between individual trimmed NURBS patches, a finite element solver needs to make sure, that certain mechanical properties, like stresses, strains and bending moments, are consistently transferred from one patch to the other across the common interface.

Breitenberger et al. [2] introduced the Isogeometric B-Rep Analysis (IBRA), which allows finite element analysis directly on B-Rep CAD models. For this, special interface elements are developed based on a classical penalty approach. As the method was initially developed for implicit static analysis based on thin Kirchhoff-Love type isogeometric shell elements, Leidinger et al. [3] extended the IBRA concept to nonlinear explicit dynamics, using shear deformable isogeometric shells available within LS-DYNA. The capabilities were demonstrated using the user-defined element interface in LS-DYNA. Inspired by the promising results, the proposed mechanical coupling method has been recently implemented into LS-DYNA and extended to rotation free thin shell isogeometric shell formulations.

The paper will be organized as follows:

Some very basic aspects of the boundary representation method used in CAD as well as some fundamentals of B-splines and NURBS surfaces will be sketched in section 2. Section 3 describes the

mechanical coupling strategy, including the formulation of the interface constraints in a strong form, its translation into a weak, integral form and some important aspects for the necessary numerical integration procedure after discretization. A rotational constraint formulation is given for the coupling of thin, rotation-free isogeometric shell formulations. Two numerical examples are presented in section 4 to demonstrate the performance of the implemented coupling strategy in LS-DYNA. The paper closes with a summary and an outlook.

2 Boundary Representation in CAD

This section will briefly summarize and introduce some basic concepts and definitions of B-Rep CAD, including B-splines and NURBS, trimming and topology.

2.1 NURBS

Instead of using low order Lagrange polynomials for the approximation of the geometry and the displacement field in an isoparametric finite element approach, non-uniform rational B-splines (NURBS) are utilized. Some basic properties of NURBS will be sketched in the following. For a deeper study on NURBS, the interested reader is referred to the monograph by Piegl and Tiller [4].

2.1.1 B-Splines

As already obvious from its name, NURBS are built from B-spline basis functions (see Fig.1) which are constructed recursively until the desired degree of the functions is reached (see Eq. (1)).

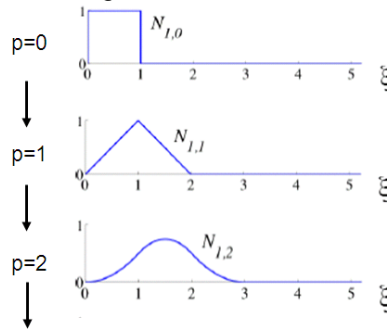


Fig. 1: B-spline basis functions of order 0, 1 and 2 for uniform knot vector [5]

The recursion formula is given by

$$\begin{aligned} \text{for } p = 0: \quad N_{i,0}(\xi) &= \begin{cases} 1 & \text{if } \xi_i \leq \xi < \xi_{i+1} \\ 0 & \text{otherwise} \end{cases} \\ \text{for } p > 0: \quad N_{i,p}(\xi) &= \frac{\xi - \xi_i}{\xi_{i+p} - \xi_i} N_{i,p-1}(\xi) + \frac{\xi_{i+p+1} - \xi}{\xi_{i+p+1} - \xi_{i+1}} N_{i+1,p-1}(\xi) \end{aligned} \quad (1)$$

where ξ_i is the i^{th} knot of the so-called “knot vector” $\Xi = [\xi_1, \xi_2, \dots, \xi_{n+p+1}]$, which is a non-decreasing set of coordinates in the parametric space, p is the order, and n is the number of basis functions. Regardless of the degree, B-spline basis functions are always positive, they constitute the important partition of unity property, and exhibit a C^{p-1} -continuity along the internal element boundaries if no multiple knot values are present in the knot-vector.

B-spline curves are created using *control points* B_i , which are used as coefficients of the B-spline basis functions. It has to be noted, that the control points are normally not part of the actual geometry which stems from the non-interpolatory nature of the B-spline basis functions. A B-spline curve $C(\xi)$ is defined through a linear combination of the B-spline basis functions with the corresponding control points.

$$C(\xi) = \sum_{i=1}^n N_{i,p}(\xi) B_i \quad (2)$$

B-spline curves may be refined (h-, p- and k-refinement) without changing the initial curve geometry.

2.1.2 NURBS surfaces

A projective transformation of a B-spline leads to a NURBS. This is achieved by introducing weights w_i at the control points. NURBS basis functions $R_i^p(\xi)$ are constructed as follows:

$$R_i^p(\xi) = \frac{N_{i,p}(\xi) w_i}{W(\xi)} \quad \text{with} \quad W(\xi) = \sum_{k=1}^n N_{k,p}(\xi) w_k \quad (3)$$

A NURBS curve is then defined in the same way as a B-spline curve, i.e. by substituting the B-spline basis functions in Eq. (2) with the NURBS basis functions.

Similarly to NURBS curves, NURBS surfaces in space can be defined. The necessary basis functions are constructed using a tensor product on the univariate basis functions (see Eq. (4)), and the final NURBS surface is then again defined through a linear combination of these basis functions with the connected control points (see Fig.2).

$$R_{i,j}^{p,q}(\xi, \eta) = \frac{N_{i,p}(\xi)M_{j,q}(\eta)w_{i,j}}{W(\xi, \eta)} \quad \text{with} \quad W(\xi, \eta) = \sum_{k=1}^n \sum_{l=1}^m N_{k,p}(\xi) M_{l,q}(\eta)w_{k,l} \quad (4)$$

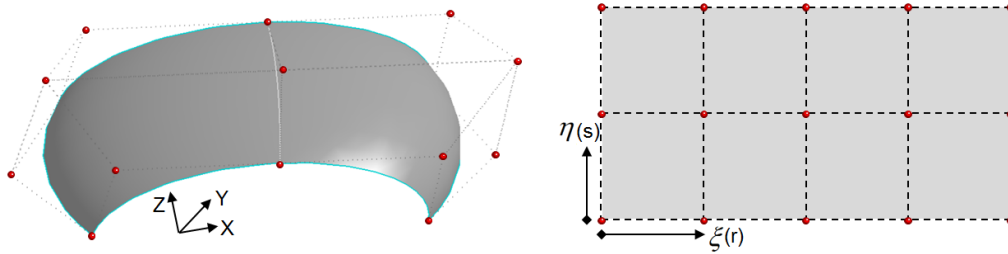


Fig.2: NURBS surface with control points in physical (left) and parametric space (right)

2.1.3 Trimmed NURBS surfaces

So far the construction of regular or standard NURBS surfaces has been discussed. But most of the time so-called *trimmed NURBS surfaces* are used in CAD packages. In addition to the definition of the NURBS surface, one or more trimming curves may be defined to trim unnecessary parts away from the initial regular patch (see Fig.3).

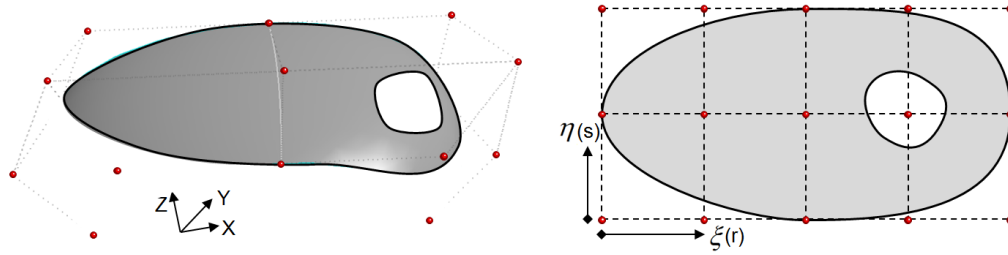


Fig.3: Trimmed NURBS surface with control points in physical (left) and parametric space (right)

2.2 Topology

To understand the concept of B-Rep in CAD, additional geometrical entities and different spaces need to be introduced. Fig.4 shows two trimmed NURBS patches together with their underlying geometric description. In CAD, the underlying (untrimmed) NURBS patch is called a surface (S), whereas the trimmed and visible part is called a face (F). The trimming curves $\bar{C}(\bar{\xi})$ are defined with respect to its underlying surface description, i.e. in the parametric space of the untrimmed NURBS patch which is given by its knot vector definition $\Xi(\xi)$ and $H(\eta)$ (see Fig.4c).

$$\bar{C}(\bar{\xi}) = \left\{ \begin{array}{l} \xi(\bar{\xi}) \\ \eta(\bar{\xi}) \end{array} \right\} = \sum_{i=1}^n N_{i,p}(\bar{\xi}) \bar{B}_i(\xi, \eta) \quad (5)$$

where $\bar{\xi}$ is the 1D trimming curve parameter, ξ and η are the corresponding 2D parametric coordinates within the underlying patch definition, and \bar{B}_i are the control points of the curve, given in the 2D parametric space as well. The parametric curve $\bar{C}(\bar{\xi})$ can be mapped to the physical (geometry) space to get $C(\xi)$ (see Fig.4a).

To define a trimming operation, trimming curves are grouped together in directed, closed trimming loops. While a counter-clockwise orientation represents an outer trimming loop, a clockwise orientation defines inner loops (holes). In the example shown in Fig.4a, it can be seen, that the two trimmed patches have a common interface represented by the trimming curves C_2 and C_9 on the first and second patch, respectively. Since the trimming curves are defined in the parametric space of their respective NURBS surface, their image in the physical space only approximately match in general. Therefore, the two trimming curves C_2 and C_9 are linked to the edge E_2 (Fig.4b), which in its essence,

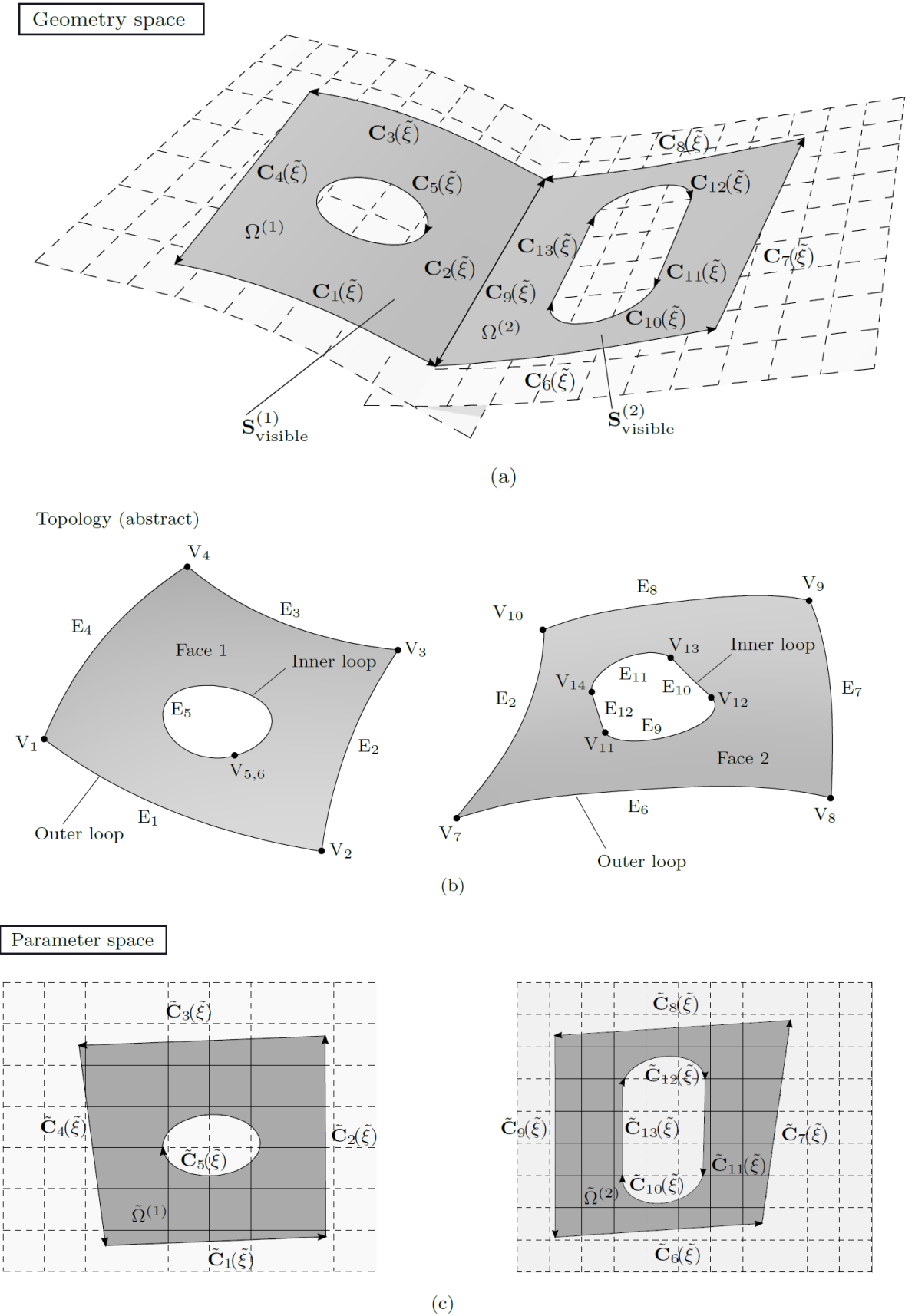


Fig.4: Trimmed surface B-Rep model represented in geometry space, as abstract topology and in parameter space, taken from Leidinger et al. [3]

establishes the topological connection between the two adjacent patches. It is worth noting that for most B-Rep CAD models, the interface between topological connected trimmed patches is not watertight and may have gaps and overlaps.

3 Mechanical coupling

In the previous section we outlined some ideas of the B-Rep definition used in CAD, including the methodology to define topological information. In order to perform numerical analysis directly on this kind of CAD representation, an isogeometric finite element solver needs to have the capability to mechanically couple the individual faces, i.e. trimmed or untrimmed NURBS patches, along their topologically defined common interfaces. Some basic ideas of a possible coupling algorithm will be given in this section. More details can be found in [2], [3], and [6].

3.1 Interface condition – strong form

Without any lack of generality, the following algorithm will be presented for a coupling interface of two adjacent faces. Along their common interface, mechanical properties shall be transmitted from one patch to the other, therefore the following conditions in the interface shall be fulfilled:

- The displacements and rotations shall be the same on both sides of the interface

In a strong form, this can be written as:

$$\mathbf{u}_1 = \mathbf{u}_2|_{\Gamma} ; \quad \boldsymbol{\theta}_1 = \boldsymbol{\theta}_2|_{\Gamma} \quad (6)$$

where Γ represents the interface.

3.2 Interface condition – penalty, weak form

Using a penalty type formulation, the strong interface conditions can be translated into a weak, integral form:

$$\alpha^{disp} \int_{\Gamma} (\mathbf{u}_1 - \mathbf{u}_2) \cdot (\delta \mathbf{u}_1 - \delta \mathbf{u}_2) d\Gamma = 0 \quad (7)$$

$$\alpha^{rot} \int_{\Gamma} (\boldsymbol{\theta}_1 - \boldsymbol{\theta}_2) \cdot (\delta \boldsymbol{\theta}_1 - \delta \boldsymbol{\theta}_2) d\Gamma = 0 \quad (8)$$

In here α^{disp} and α^{rot} are the penalty factors for enforcing the displacement and rotational constraints and $\delta \mathbf{u}$ and $\delta \boldsymbol{\theta}$ are variations of the continuous displacement and rotation fields, sometimes also called “virtual displacements and rotations” in the context of the principle of virtual work.

3.3 Discretization

In the isogeometric finite element analysis framework used here, the continuous fields $(\mathbf{u}, \boldsymbol{\theta}, \delta \mathbf{u}, \delta \boldsymbol{\theta})$ are discretized using NURBS basis functions. Furthermore the discretized versions of the weak forms given in Eq. (7) and (8) have to be numerically integrated along the common interface. To do so, the integration domain along the interface is split into a set of non-overlapping, so-called B-Rep edge elements [2]. Similar to standard contact algorithms, one side of the interface is chosen to be the master side, on which the numerical integration is performed. Thus, necessary terms including shape functions and their derivatives need to be mapped from the parameter space of the slave side to the one on the master side. Fig.5 shows the necessary mapping procedure to define the B-Rep edge elements on the master curve. A B-Rep edge element e_i is defined between any two consecutive points (either black or red) shown on the right side of Fig.5.

Once the numerical integration in the B-Rep edge elements is performed, equivalent penalty forces and stiffnesses (for implicit analysis) for the involved control points are computed and assembled to the global force vector and stiffness matrix if necessary. For additional details the interested reader is referred to the detailed descriptions given in [2], [6], and [3].

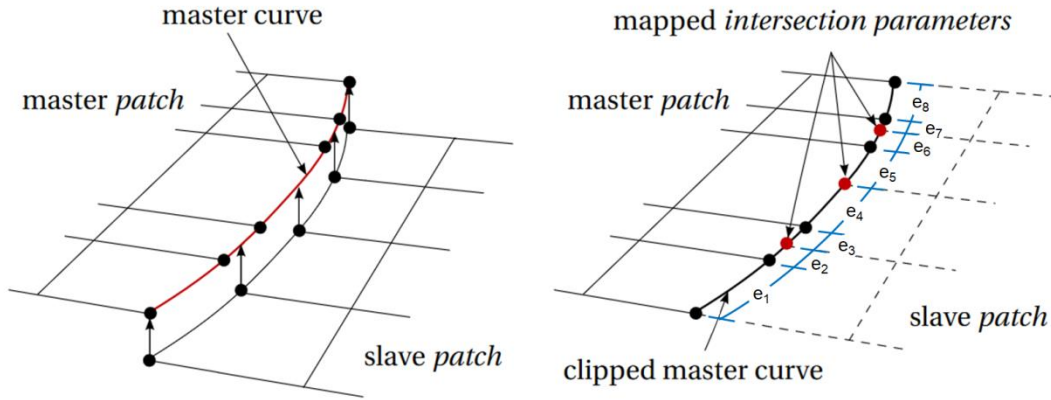


Fig.5: Mapping from slave curve onto master curve to define B-Rep edge elements [6].

3.4 Rotational constraints

The enforcement of the translational constraint (Eq. (7)) is rather straightforward, while the enforcement of the rotational constraint (Eq. (8)) need some additional comments. In LS-DYNA isogeometric shell formulations are available that are based on the shear deformable Reissner-Mindlin as well as the thin Kirchhoff-Love shell theory with and without rotational degrees of freedom (DOFs) at their control points. In case of the shear deformable shell formulation, the rotational interface constraint enforcement can be directly related to the rotational degrees of freedom. For thin shell element formulations, no rotational DOFs are introduced, thus the rotational constraint is enforced in a somewhat different way.

3.4.1 Rotation-free shell formulations

The enforcement of the rotational interface constraints in case of rotation-free shell formulations is based on the ideas presented by Benson et al. [7]. A total Lagrangian constraint formulation is utilized:

$$\sin(\theta - \theta_0) = \sin(\theta)\cos(\theta_0) - \cos(\theta)\sin(\theta_0) = 0; \quad \cos(\theta) = \mathbf{n}_1 \cdot \mathbf{n}_2 \quad \text{and} \quad \sin(\theta) = \mathbf{t} \cdot \mathbf{n}_1 \otimes \mathbf{n}_2 \quad (9)$$

In here θ_0 and θ represent the initial and the current angle at the interface, \mathbf{n}_1 and \mathbf{n}_2 are the surface normal vectors of the two joining patches at the interface, and \mathbf{t} is the tangent vector at the interface curve. The constraint expression given in Eq. (9) is evaluated at the integration points of the B-Rep edge elements and numerically integrated along the interface.

4 Examples

Two examples are presented to demonstrate the functionality of the proposed coupling strategy. The first one is a simple curved shell structure that could be easily discretized with one single untrimmed NURBS patch. Taking the single patch result as the reference solution, the resulting displacement fields for various multi-patch trimmed NURBS discretizations are compared. Furthermore, the performance of the rotational constraint enforcement is analyzed using rotation-free shell elements. The second example uses a small subsection of a rather typical B-Rep CAD structure to demonstrate the coupling behavior in a 3 point bending test.

4.1 Impact on a curved shell

The first example is chosen to compare the deformation of a simple curved shell structure that is hit by an impactor when discretized either with one simple untrimmed NURBS patch or with multiple, mechanically coupled trimmed NURBS patches. In Fig.6 left, the shell is shown discretized with a single, untrimmed NURBS patch, together with the impactor and the single point constraints at the four corner control points. A simple elasto-plastic material model is used for all the computations.

For the simplest case of dividing the shell into two trimmed patches, the trimming curves C_{xx} and the physical edge E_1 are displayed on the right in Fig.6. The physical edge E_1 represents the trimming curve C_{12} for the patch on the left side of the interface as well as the trimming curve C_{24} for patch on the right side of the interface and thus, implicitly defines the topological connection between the two patches.

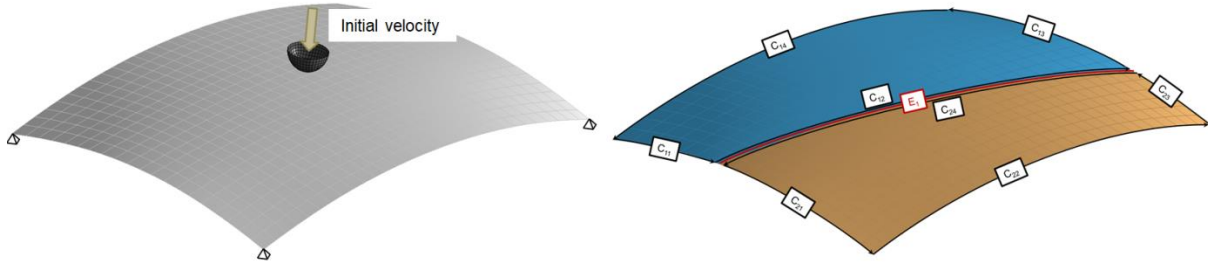


Fig.6: Left: simply supported shell and impactor with initial velocity
Right: trimming curves for subdividing the shell into two trimmed patches

In the multi-patch discretizations, different refinement levels have been chosen within the individual patches to make sure that we end up with non-matching grids along the coupling interfaces (Fig.7). For all cases, bi-quadratic NURBS have been used.

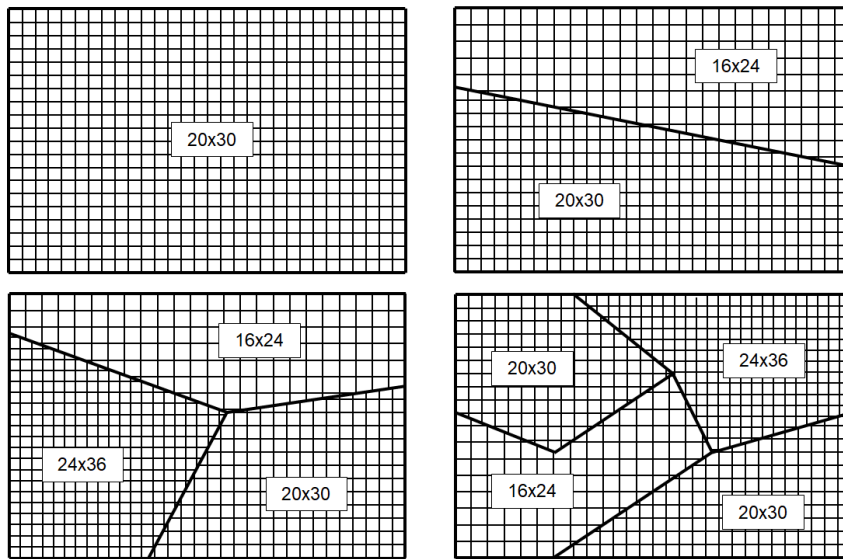


Fig.7: Discretization of the different cases, the subdivisions relate to the full, untrimmed patch

In Fig.8 fringe plots of the resulting displacement fields are shown for the untrimmed, single NURBS patch case together with the other three multi-patch trimmed NURBS patch discretizations. For this first study, shear deformable Reissner-Mindlin type isogeometric shell elements are used..

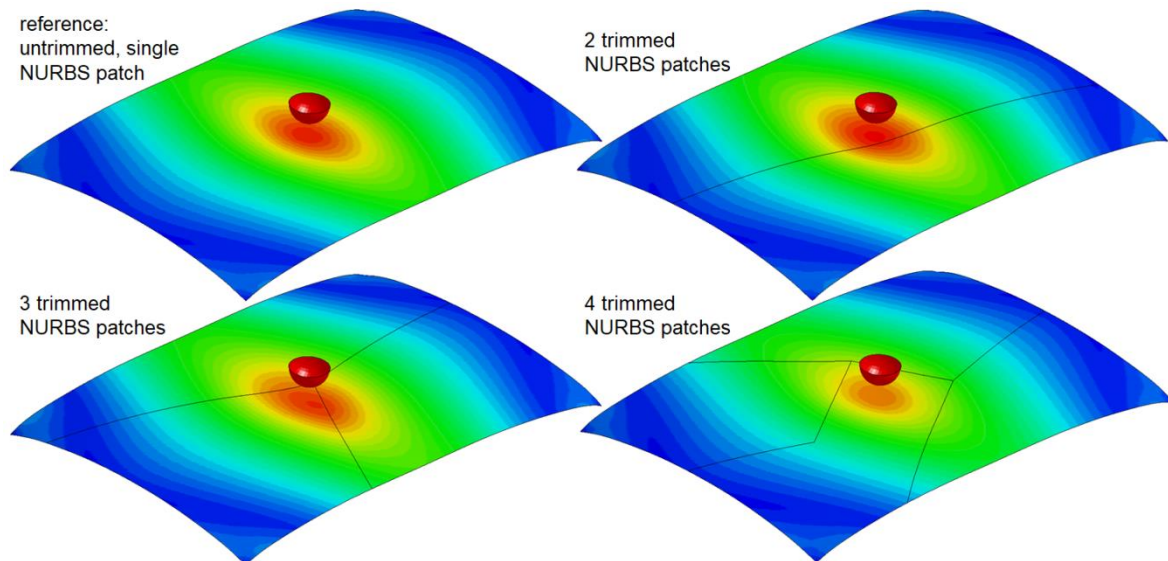


Fig.8: Resultant displacement field at simulation time $t=17.5$ for shear deformable Reissner-Mindlin shell element (FORM=0 in *ELEMENT_SHELL_NURBS_PATCH)

Looking at the resulting displacement fields it is obvious that the coupling strategy makes sure, that we have a smooth transition of the displacement field across the coupling interfaces. However it can be seen, that the number of coupling intersections may have some impact on the overall results. The maximum displacements at the given simulation time differed in the range of 2.5% compared to the reference solution. This difference is clearly a result of the coupling but also the different refinement levels in the trimmed patches may have an influence here. Furthermore, the choice of the penalty stiffness influences the quality of the constraint enforcement.

To study the performance of the rotational constraint enforcement in case thin, rotation-free isogeometric shell elements are being used, the element formulation has been switched to FORM=1 (`*ELEMENT_SHELL_NURBS_PATCH`). Again, Fig.9 displays the resulting displacement fields at a certain simulation time. The constraints seem to work properly as there is a smooth transition across the coupling interface. However, the absolute value of the displacement differ slightly in the case with four trimmed patches, which could be due to the different refinement levels used.

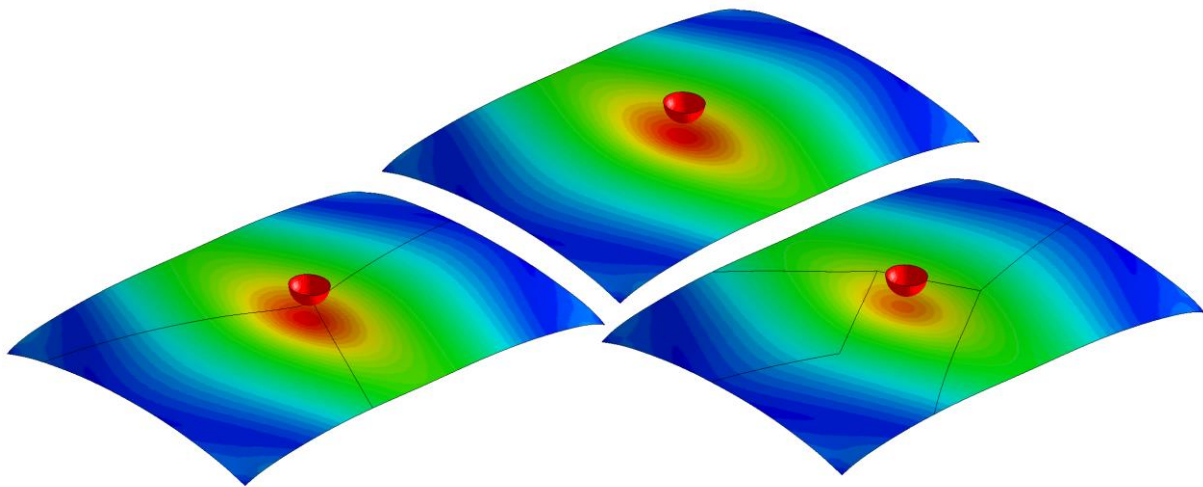


Fig.9: Resultant displacement field at simulation time $t=17.5$ for thin Kirchhoff-Love shell element (FORM=1 in `*ELEMENT_SHELL_NURBS_PATCH`) and active rotational constraint enforcement

In order to clearly demonstrate the effect of the additional rotational constraint enforcement in case of thin, rotation-free shell elements, the rotational constraint enforcement has been deactivated. The results for this case are shown in Fig.10. Note that the translational constraints are still nicely enforced but the lack of having an active rotational constraint enforcement leads to very pronounced kinks along the coupling interface and weakens the whole structure dramatically.

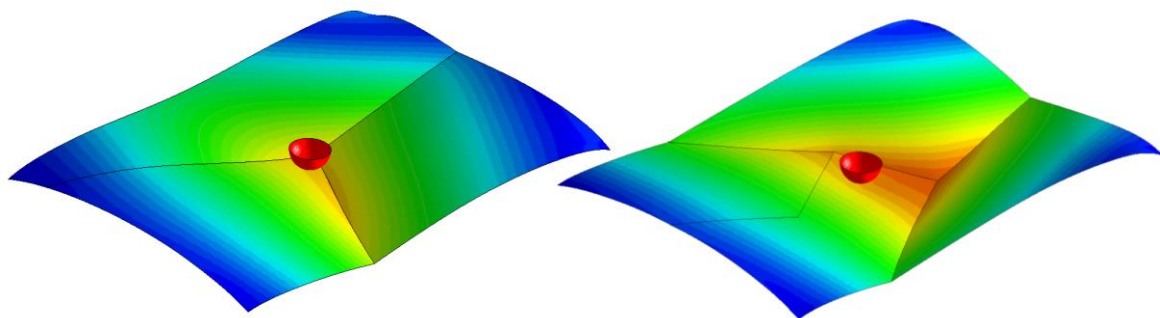


Fig.10: Resultant displacement field at simulation time $t=17.5$ for thin Kirchhoff-Love shell element (FORM=1 in `*ELEMENT_SHELL_NURBS_PATCH`) without rotational constraint enforcement

4.2 3 point bending test

In the second example a substructure of a quite realistic B-Rep CAD model is analyzed by a 3 point bending test (see Fig.11). The part consists of 24 trimmed NURBS patches that are joined along their topologically defined interfaces via the presented coupling strategy. Shear deformable isogeometric shell elements (FORM=0) have been used for the discretization of the part. The support as well as the impactor has been modeled with standard bi-linear shell elements. A simple elasto-plastic material model has been used.

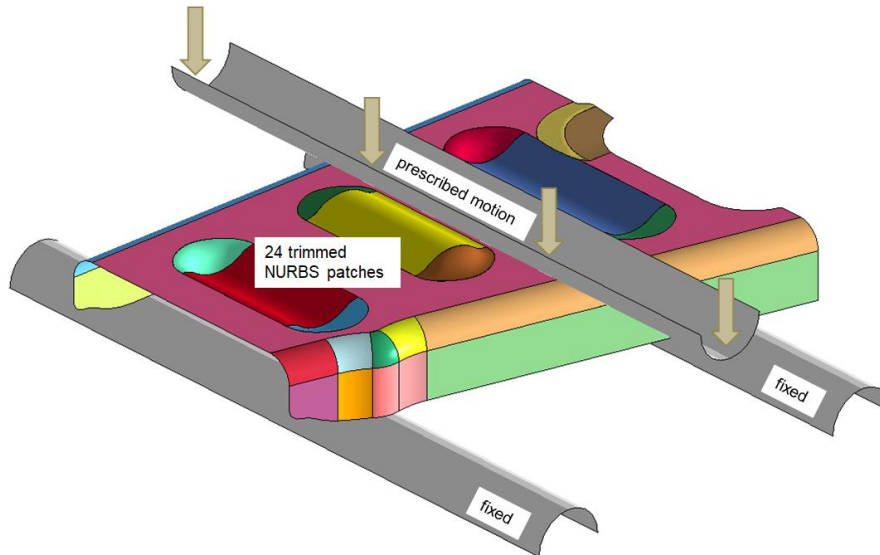


Fig.11: Setup of 3 point bending test

In Figs.12 and 13 the deformation of the part is shown. Again, the fringe plots of the deformation field show a nice and smooth transition of the displacements across all present coupling interfaces.

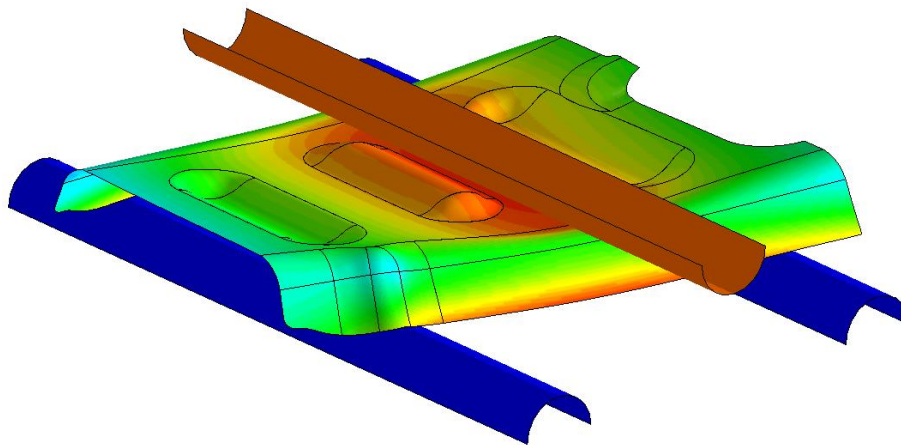


Fig.12: Deformed configuration

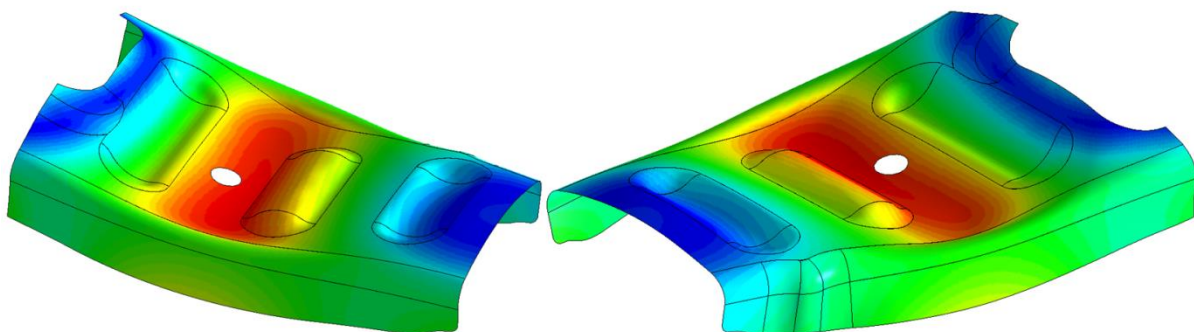


Fig.13: Deformed part (displacements scaled by a factor of 5)

5 Summary

A strategy to mechanically couple topologically connected multi-patch trimmed NURBS shells in LS-DYNA has been presented. The concept is mainly based on the works by Breitenberger et al. [2] as well as Leidinger et al. [3] and uses a weak constraint enforcement across the common interfaces based on a classical penalty approach. Two numerical examples have been analyzed to demonstrate the performance of the presented strategy. Although these first results are very promising, further studies on more realistic and complex geometries are necessary to improve the stability and quality of this coupling method.

6 Literature

- [1] Hughes, T.J.R., Cottrell, J.A., Bazilevs, Y.: "Isogeometric Analysis: CAD, finite elements, NURBS, exact geometry, and mesh refinement", *Computer Methods in Applied Mechanics and Engineering*, 194, 2005, 4135-4195.
- [2] Breitenberger, M., Apostolatos, A., Philipp, B., Wüchner, R., Bletzinger, K.-U.: "Analysis in computer aided design: Nonlinear isogeometric B-Rep analysis of shell structures", *Computer Methods in Applied Mechanics and Engineering*, Vol. 284, 2015, 401-457.
- [3] Leidinger, L.F., Breitenberger, M., Bauer, A.M., Hartmann, S., Wüchner, R., Bletzinger, K.-U., Duddeck, F., Song, L.: "Explicit Dynamic Isogeometric B-Rep Analysis of Penalty-Coupled Trimmed NURBS Shells", Submitted to *Computer Methods in Applied Mechanics and Engineering*, 2019.
- [4] Piegl, L., Tiller, W.: "The NURBS Book", Springer-Verlag (Berlin-Heidelberg), 1995.
- [5] Cottrell, J.A., Hughes, T.J.R., Bazilevs, Y.: "Isogeometric Analysis – Toward Integration of CAD and FEA", John Wiley & Sons, Ltd, 2009.
- [6] Breitenberger, M.: "CAD-integrated design and analysis of shell structures", PhD Thesis, Technical University of Munich, 2016.
- [7] Benson, D., Nagy, A., Hartmann, S.: "Tied Contact for Explicit Dynamics with Isogeometric Analysis", 13th U.S. National Congress on Computational Mechanics, San Diego, California, USA, July 27-30, 2015.